Layer Resolved Structural Relaxation at the Surface of Magnetic FePt Icosahedral Nanoparticles

R. M. Wang,[1,2,*] O. Dmitrieva,[3] M. Farle,[3,†] G. Dumpich,[3] H. Q. Ye,[4] H. Poppa,[2] R. Kilaas,[2] and C. Kisielowski[2,‡]

[1]*School of Science, Beijing University of Aeronautics and Astronautics, Beijing 100083, People's Republic of China*
[2]*National Center for Electron Microscopy, Lawrence Berkeley National Laboratory, University of California, Berkeley, California 94720, USA*
[3]*Fachbereich Physik and Center for Nanointegration, Universität Duisburg-Essen, 47048 Duisburg, Germany*
[4]*Department of Physics, Peking University, Beijing 100871, People's Republic of China*

(Received 10 July 2007; published 10 January 2008)

The periodic shell structure and surface reconstruction of metallic FePt nanoparticles with icosahedral structure has been quantitatively studied by high-resolution transmission electron microscopy with focal series reconstruction with sub-angstrom resolution. The icosahedral FePt nanoparticles fabricated by the gas phase condensation technique in vacuum have been found to be surprisingly oxidation resistant and stable under electron beam irradiation. We find the lattice spacing of (111) planes in the surface region to be size dependent and to expand by as much as 9% with respect to the bulk value of $Fe_{52}Pt_{48}$. Controlled removal of the (111) surface layers *in situ* results in a similar outward relaxation of the new surface layer. This unusually large layerwise outward relaxation is discussed in terms of preferential Pt segregation to the surface forming a Pt enriched shell around a Fe-rich Fe/Pt core.

DOI: 10.1103/PhysRevLett.100.017205 PACS numbers: 75.50.Bb, 75.25.+z, 75.50.Ss, 75.75.+a

The structure of small particles is a topic which has attracted interest for more than a century [1]. Icosahedral-shaped particles can be described as a platonic solid in which each tetrahedron is distorted. Such noncrystallographic structures were called multiply twinned particles or MTPs. There are substantial discussions as to their growth mechanism [2]. Recently, increasing evidence was gathered that nanoparticles and clusters possess ''shell periodicity'' and grow by the accretion of atomic layers. The shell periodicity imposes certain restrictions on the symmetry of the clusters following Plato's five geometric bodies [3–5]. Excellent examples of such shell structures are Mackay icosahedra [6], which are composed of 20 twin-related tetrahedra packed along (111) faces as is shown in Fig. 1(a). It is seen from the geometrical model that an elastic deformation of the individual tetrahedra is required, if merged into icosahedra, which is why one expects that such particles are compressed. However, despite numerous studies on their structure (see, for example, [3–5]), no direct experimental evidence of such shell formation or compression from atomically resolved images has been reported. A topic which is of similar interest—but one that has been hardly addressed—is the question of whether surface reconstructions occur on nanoparticle surfaces the same way as in the bulk [7]. Localized lattice relaxations or surface reconstructions of individual nanoparticles have not been reported either because of limitations of previous transmission electron microscopy (TEM) studies [8–10]. Recent advances in TEM imaging approaches such as the reconstruction of electron exit waves from focal series of lattice images extend the resolution to the sub-angstrom regime to correct for dominant aberrations of the objective lens [11,12]. This has enabled us to directly explore the lattice structure and reconstruction in the surface region of FePt icosahedra with lateral dimensions of only 9 to 11 atoms.

For our investigation we chose the bimetallic alloy FePt, which—due to its large magnetic anisotropy density—has been identified as the best candidate for the fabrication of future ultrahigh density magnetic recording media based on self-assembled arrays of magnetic nanoparticles (NPs). These have been synthesized using organometallic chemistry or gas phase condensation methods [13]. The latter method affords the possibility to form differently shaped nanoparticles such as icosahedra, decahedra, and cuboctahedra and also larger facetted spheres [14]. The transformation to the $L1_0$ phase in FePt NPs smaller than 4 nm has never been unambiguously identified, and the possibility of its formation in small NPs has been questioned based on the influence of surface composition and segregation [15]. Commonly in these discussions, a uniform crystal structure across the NP is assumed; that is to say, the influence of a

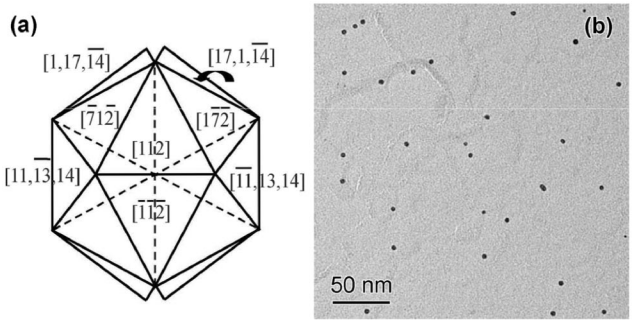

FIG. 1. (a) Formation of an icosahedron by a suitable combination of 20 tetrahedra, compressive strain is required to accommodate the tetrahedra. (b) Distribution of the FePt nanoparticles in standard bright field TEM.

possible relaxation of the surface layers as is known at the surface of bulk crystals or surface segregation phenomena known in $Pt_{80}Fe_{20}$ films has not been considered. Here, we show that layerwise surface relaxations of up to ~9% with respect to the bulk spacings indeed exist at the (111) facets of icosahedral FePt NPs. This is attributed to the energetically favored formation of a Pt enriched surface region which in turn prevents the formation of the stoichiometric $Fe_{50}Pt_{50}$ $L1_0$ ordered state in the particle.

FePt NPs with diameters of 5–6 nm were formed in the gas phase by a dc-sputtering process in a continuous gas flow of Ar (99.999%) and He (99.999%) at pressures of 0.5 to 1 mbar [16]. In this approach the particles are formed first and subsequently annealed at $T_s = 1073$ K while flying through a heated vacuum tube before being deposited onto amorphous carbon grids fixed on a liquid nitrogen cooled substrate holder. To prevent the particles from oxidation during formation, the vacuum system is designed to meet ultrahigh vacuum standards (pressure $p = 10^{-7}$ Pa). An alloy target with a composition of $Fe_{55}Pt_{45}$ was used, and the average composition of individual particles was measured to be $Fe_{52}Pt_{48}$ with an error of ±2%. Details of the analysis and the gas phase synthesis have been published previously [14,16].

Focal series of high-resolution TEM lattice images were recorded with a Philips CM300 FEG/UT instrument and reconstructed as described earlier to obtain the amplitude and phase of the electron wave exiting the particles [17,18]. Using this exit wave reconstruction technique a resolution of 0.08 nm can be obtained [19]. Additional image simulations of the transmission electron contrast for model particles were carried out with the MacTempas software [20]. Finally, we can pinpoint atom column positions by fitting model functions to the intensity maxima of electron exit waves (phase images) with a precision of 0.1 pixel [21].

Bright field TEM and Z-contrast scanning transmission electron microscopy images of the nanoparticles on carbon support films show homogenously distributed particles with identical sizes of about 5–6 nm [Fig. 1(b)]. Figure 2 shows exit wave phase images of one representative FePt nanoparticle that were reconstructed from 3 successive focus series each consisting of 20 lattice images. In total, more than 10 icosahedra of equal size were analyzed in the same extensive way by two different microscopists, and the same results were obtained within experimental error. The images of Fig. 2 show well-resolved {111} and {220} planes with spacing of 0.220 and 0.135 nm of the fcc FePt structure (space group $Fm3m$, $a = 0.3816$ nm). The upper and lower parts of the phase are structural projections of tetrahedra viewed along ⟨110⟩ directions, while the left and right parts correspond to views along ⟨111⟩ directions. The complex fringes in the center were determined as belonging to a projection along ⟨112⟩.

The acquisition time for one focal series of 20 lattice images was ~100 s. The current density at the sample was

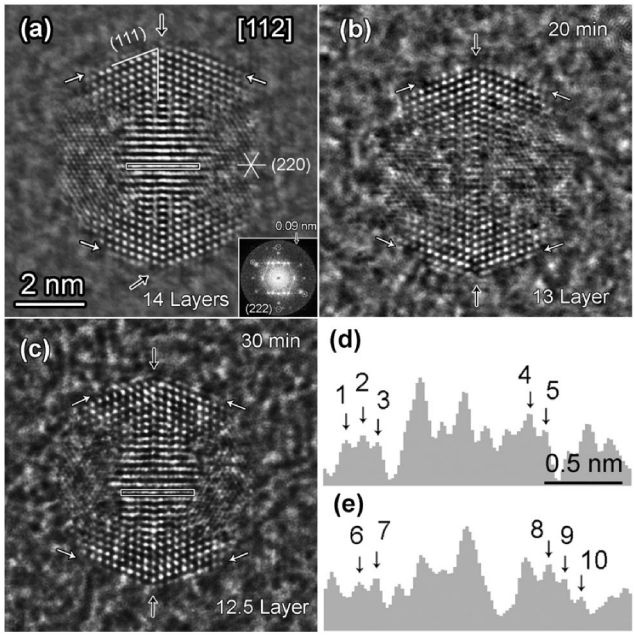

FIG. 2. Experimental exit wave phase images of the same representative FePt nanoparticle exposed to a current density of ~20 A/cm^2 at 300 kV for 0, 20, and 30 min [panels (a), (b), and (c), respectively]. White arrows mark partially occupied shells. Dark arrows mark edge columns that are commonly missing. The inset of (a) is a Fourier transform of the phase image showing an information limit of 0.090 nm. Note the successive removal of the surface layers effectively reducing the size of the particle. Panel (d) shows line profiles taken from the indicated areas of the real space images. Details as narrowly spaced as 0.09 nm can be resolved.

measured to be ~20 A/cm^2 at 300 kV. It is remarkable to find that under such conditions the FePt nanoparticle was stable. With extended electron beam irradiation time, it was found that the structure of the FePt MTP remained icosahedral. However, the diameter of the particle shrank during the successive recordings, and by analyzing Figs. 2(a) and 2(c) we find a reduction of the particles diameter with irradiation time that is characterized by a decreasing number of shells, which are 14, 13, and 12.5 for the successive recordings. Therefore, the electron beam "peels" the particle shell by shell at a rate of approximately 1 shell per 20 min. A further increase of the beam current results in major rotational and translational particle motions and structural fluctuations. Moreover, the large particle stability allows for a record resolution of around 0.1 nm. The inset of Fig. 2(a) shows a Fourier transformation of the corresponding phase image where the outer circle marks an information limit of 0.090 nm. Image Fourier components extend to this limit. Accordingly, intensity profiles [Fig. 2(d)] reveal resolvable distances that can be as small as 0.09 nm. It follows, therefore, that subangstrom resolution can be obtained not only from suitably prepared bulk materials but also from complex crystallographic nanostructures.

In the reconstructed phase image, the intensity maxima mark atom columns that can be analyzed in terms of column positions and heights (sample thickness). The low intensities indicate that the corresponding atomic columns are only partially filled, as indicated by white arrows. The intensities of edge columns (marked by black arrows) are much lower or even absent, proving that whole columns can be removed from these sites.

The particle structure described above must be interpreted in terms of a multiply twinned model as first proposed by Ino [1] and is depicted in Fig. 3(a). Initially, the 10 179 Fe and Pt atoms were distributed statistically according to their chemical ratio (52:48) to simulate a phase image. The geometrical structure model was shell growth icosahedron. The corresponding simulated phase image of exit waves is shown in Fig. 3(b) and it compares well with the measurements of Fig. 2, proving that the particle is an icosahedral MTP. Residual differences relate to an imperfect alignment of the particles zone axes with the electron beam and surface relaxation as indicated below.

A quantitative evaluation of strain relaxation processes is possible by extraction of column position maps from the experiments. Here, one must also consider the possibility that there may be buckling of atoms in the atomic columns which might cause an anisotropic smearing of the intensity profile of the respective column. Within our resolution such anisotropic intensity is not observed, and we can recover the centers of such columns from the experiment by fitting model functions to intensity maxima [21]. Four image parts A, B, C, and D must be distinguished because of the different orientation of the particle forming tetrahedra. The {111} layer spacing can be measured in each part. Averaging equivalent sites in the four symmetrical parts minimizes errors originating from the misorientation with respect to the zone axes and the above mentioned buckling within atomic columns of the particle. Figure 4(a) is a position map from the particle shown in Fig. 2(a), and the spacing between shells n and $n+1$ is plotted in Fig. 4(b) where $n = 0$ marks the difference between the outermost and the first shell, which is 0.231 ± 0.004 nm.

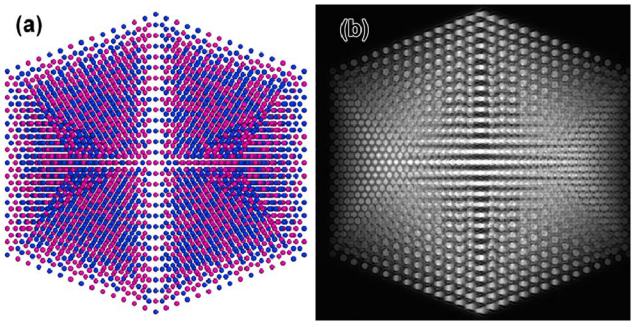

FIG. 3 (color online). Modeling and simulations. (a) Proposed icosahedron model with 10 179 randomly distributed Fe and Pt atoms. (b) Simulated phase image from the proposed model matches the experiments from Fig. 2.

Application of the same procedure to the images of Figs. 2(b) and 2(c) reproduces the result within experimental error, with an indication that a smaller occupancy of the outermost layer results in a larger spacing. In addition, we measured the spacing between the {111} planes parallel to the twinning planes and mean values from the three image sets. Results shown as an inset of Fig. 4(b) indicate that the entire nanoparticle expands with decreasing particle size. The origin of this expansion in smaller particles is not clear and is most likely related to changes of the electronic structure and the increased surface-to-volume ratio which changes the balance of elastic energies in the multiply twinned particle. It is most unexpected to see in Fig. 4(b) that the spacing between the shells decreases exponentially with shell numbers [e.g., $d_{111}(n) = 0.2113 + 0.0204e^{-n/1.8}$ nm] resulting in ~9.4% outward relaxation of the surface layer ($n = 0$) when compared to the spacing of the inner layers $n = 3$ to 6. Comparison with the lattice structure of fcc $Fe_{52}Pt_{48}$ ($d_{111}{}^{\mathrm{fcc}} = 0.2198$ nm) reveals that the surface is under tensile strain by 6% (9% for the smaller icosahedra) and the inner shells ($d_{111} = 0.213$ nm) are compressed by 3%.

The compression of the inner layers relative to the bulk value could be understood when one assumes that the core of the icosahedra is Fe rich; that is, the core composition may approach that of $Fe_{80}Pt_{20}$ which has a 3% reduced d_{111} spacing. Such an outward segregation of Pt would reduce compressive strain. Also, the well-known compression of the (111) spacings, $d_{111}{}^{\mathrm{ico}} = 0.973 d_{111}{}^{\mathrm{fcc}}$, in single element icosahedra may also be an explanation. At the particle surface, the measured spacing even exceeds the bulk lattice parameter of solid Pt. It is, however, very close to the spacing of the top (111) layer of a $Fe_{20}Pt_{80}$ film ($d_{111} = 0.2357$ nm) [7,22] which contains 100% Pt atoms. This shows a surface reconstruction with an outward buckling of +0.009 nm and a Pt enriched second layer. Pt segregation at crystal surfaces has been reported previously

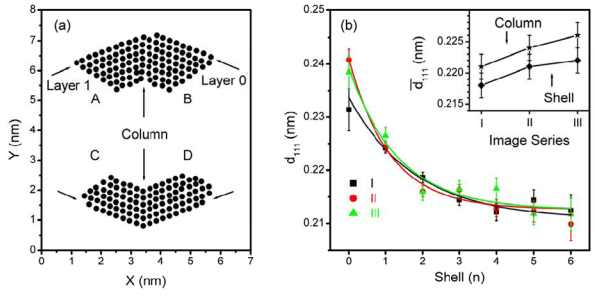

FIG. 4 (color online). Quantitative data analyses. (a) Column position map of the particle shown in Fig. 2(a). (b) Shell spacing of Fig. 2 as function of shell number. Solid lines are fitted exponential functions. The symbols I, II, and III refer to Figs. 2(a)–2(c), respectively. The smaller particle shows the largest outward d_{111} relaxation. The bulk value of $Fe_{52}Pt_{48}$ is $d_{111} = 0.2198$ nm. The inset compares the average shell and column spacing that increase as the particle shrinks.

[23,24]. Our findings suggest a partial substitution of iron atoms by Pt in the outermost shell. The presence of such a Pt enriched surface layer provides the explanation for the experimentally observed oxidation resistance of the MTPs in comparison to colloidal FePt particles. Also, the corresponding Fe enrichment of the MTP's inner layers prevents the formation of the $L1_0$ phase. During the formation of the bimetallic icosahedra in the gas phase, the diffusion of the larger Pt atoms to the topmost shells is energetically favored, thus releasing the elastic energy stored in the compressive strain of the icosahedra. Additionally, one should note that differently shaped NPs are formed when nucleated in the gas phase at different pressures of the dc-sputtering Ar gas. Higher Ar sputtering gas pressures (0.5 mbar), or in other words higher ion etching rates, may prevent the formation of icosahedra and stabilizing Pt shells—thereby transforming the MTPs during the nucleation to decahedral particles. These in turn can be transformed to the $L1_0$ phase by subsequent annealing in the gas phase.

Finally, we would like to note that already a distortion of less than 2% of a ferromagnet with cubic (fcc or bcc) structure may increase its magnetic anisotropy density by 2 orders of magnitude as, for example, evidenced in the tetragonally distorted $L1_0$ phase of FePt or in face centered tetragonal Ni films on Cu(100) [25]. Hence, the observed lattice distortion and Pt concentration gradient will cause a random magnetic anisotropy which results in a reduction of the magnetic anisotropy. As such lattice reconstruction in the surface region of nominally $L1_0$ ordered 3 to 10 nm FePt particles cannot be excluded, one could tentatively interpret the often observed too small anisotropy energies and coercive fields [14,26,27] as being due to the locally varying anisotropy fields within the particles.

In conclusion, we have quantitatively determined a size-dependent surface reconstruction and a layerwise relaxation of up to 9% in the surface region of icosahedral FePt nanoparticles, providing a possible explanation for the reduced magnetic anisotropy usually observed in FePt nanoparticles. We have also given evidence of a shell growth mechanism in the gas phase—in difference to growth in organometallic synthesis—based on the release of elastic energies. The structural results can be understood when a radial composition gradient with a Pt rich shell and a Fe-rich core is assumed, which makes the particles environmentally stable nanomagnets with a surface layer that may suppress technologically undesired magnetic exchange coupling. The observed surface reconstructions may be a general phenomenon in binary metal nanoparticles and may help one to understand differences in calculated and experimentally determined electronic and magnetic properties. High-resolution TEM images of complex nanoparticles were obtained with a resolution that breaks the 1 Å limit.

This work was supported by the Director, Office of Science, Office of Basic Energy Science, of the U.S. Department of Energy under Contract No. DE-AC02-05CH11231, the Berkeley Scholar Program, the National Natural Science Foundation of China (No. 50671003), the Program for New Century Excellent Talents in University (NCET-06-0175), and the Deutsche Forschungsgemeinschaft SFB 445. Helpful discussions with M. José-Yacamán (University of Texas—Austin, USA) are acknowledged.

*rmwang@buaa.edu.cn
†farle@uni-due.de
‡CFKisielowski@lbl.gov

[1] S. Ino, J. Phys. Soc. Jpn. **21**, 346 (1966).
[2] L. D. Marks, Rep. Prog. Phys. **57**, 603 (1994).
[3] T. P. Martin, Phys. Rep. **273**, 199 (1996).
[4] J. L. Rodriguez-Lopez *et al.*, Phys. Rev. Lett. **92**, 196102 (2004).
[5] H.-S. Nam, Phys. Rev. Lett. **89**, 275502 (2002).
[6] A. L. Mackay, Acta Crystallogr. **15**, 916 (1962).
[7] M. A. Vasiliev, J. Phys. D **30**, 3037 (1997).
[8] P. M. Ajayan and L. D. Marks, Phys. Rev. Lett. **60**, 585 (1988).
[9] S. Iijima and T. Ichihashi, Phys. Rev. Lett. **56**, 616 (1986).
[10] P. M. Ajayan and L. D. Marks, Phys. Rev. Lett. **63**, 279 (1989).
[11] C. Kisielowski *et al.*, Ultramicroscopy **89**, 243 (2001).
[12] C. L. Jia, M. Lentzen, and K. Urban, Science **299**, 870 (2003).
[13] B. D. Terris and T. Thomson, J. Phys. D **38**, R199 (2005).
[14] B. Rellinghaus *et al.*, J. Magn. Magn. Mater. **266**, 142 (2003).
[15] M. Müller and K. Albe, Phys. Rev. B **72**, 094203 (2005).
[16] S. Stappert *et al.*, J. Cryst. Growth **252**, 440 (2003).
[17] W. M. J. Coene *et al.*, Ultramicroscopy **64**, 109 (1996).
[18] A. Thust *et al.*, Ultramicroscopy **64**, 211 (1996).
[19] X. Xu *et al.*, Phys. Rev. Lett. **95**, 145501 (2005).
[20] http://www.totalresolution.com/MacTempas.html.
[21] C. Kisielowski, O. Schmidt, and J. Yang, Mater. Res. Soc. Symp. Proc. **482**, 369 (1998).
[22] P. Beccat, Y. Gauthier, R. Baudoing-Savois, and J. C. Bertolini, Surf. Sci. **238**, 105 (1990).
[23] C. Creemers and P. Deurinck, Surf. Interface Anal. **25**, 177 (1997).
[24] G. F. Wang *et al.*, J. Chem. Phys. **122**, 024706 (2005).
[25] M. Farle, Rep. Prog. Phys. **61**, 755 (1998).
[26] C. Antoniak *et al.*, Phys. Rev. Lett. **97**, 117201 (2006).
[27] C. Antoniak and M. Farle, Mod. Phys. Lett. B **21**, 1111 (2007).